Role of the Sterol Superlattice in the Partitioning of the Antifungal Drug Nystatin into Lipid Membranes[†,‡]

Mei Mei Wang,[§] Istvan P. Sugar,[||] and Parkson Lee-Gau Chong*[,§]

Department of Biochemistry, Temple University School of Medicine, Philadelphia, Pennsylvania 19140, and Departments of Biomathematical Sciences and Physiology & Biophysics, Mount Sinai Medical Center, New York, New York 10029

Received February 4, 1998; Revised Manuscript Received June 29, 1998

ABSTRACT: Nystatin isolated from *Streptomyces* is a polyene antibiotic that is frequently used in the treatment and prophylaxis of fungal infections. Here, the fractional sterol concentration dependencies of the partition coefficient for partitioning of nystatin into ergosterol/dimyristoyl-L-α-phosphatidylcholine (DMPC), cholesterol/DMPC, ergosterol/1-palmitoyl-2-oleoyl-L-α-phosphatidylcholine (POPC), and ergosterol/POPC/1-palmitoyl-2-oleoyl-L-α-phosphatidylethanolamine (POPE) multilamellar vesicles have been determined fluorometrically at 37 °C using ∼0.3−1.0 mol % sterol concentration increments over a wide concentration range (e.g., 18−54 mol % sterol). This unconventional approach of varying membrane sterol content, in contrast to previous studies using large sterol concentration increments (e.g., 10 mol %), leads to a striking observation. The partition coefficient of nystatin changes dramatically with membrane sterol content in a well-defined alternating manner, displaying a local minimum at or very close to the critical sterol mole fractions (e.g., 20.0, 22.2, 25.0, 33.3, 40.0, and 50.0 mol % sterol) predicted for sterols regularly distributed in either hexagonal or centered rectangular superlattices. In ergosterol/DMPC bilayers, for example, there is a >3-fold increase in nystatin partitioning with a minute change (∼1 mol %) in sterol content on either side of the critical sterol mole fraction, 25.0 mol %. These results provide semifunctional evidence supporting the sterol regular distribution model [Chong, P. L.-G. (1994) *Proc. Natl. Acad. Sci. U.S.A. 91*, 10069−10073]. More importantly, these results reveal a new membrane phenomenon, that is, that nystatin partitioning is affected by the extent of sterol regular distribution in the plane of the membrane. This phenomenon occurs not only in saturated (e.g., DMPC) but also in unsaturated (e.g., POPC) lipid membranes, and persists in the presence of polar headgroup heterogeneity (e.g., POPC/POPE). This membrane property points to a new method for studying the interactions of polyene antibiotics with sterol-containing membranes, and the need to consider the membrane sterol content of the target cells when administering nystatin or other polyene antibiotics.

Polyene macrolide antibiotics are a family of compounds characterized by a large lactone ring, which contains three to eight conjugated double bonds. Among this family, nystatin and amphotericin B are most important because they are frequently used in the treatment and prophylaxis of life-threatening fungal infections (*1*−*5*). These two antibiotics, isolated from the same species *Streptomyces nodosus*, possess similar structures; the major difference is that amphotericin B has a heptaene, whereas nystatin contains a tetraene and a diene in the polyenic chain separated by a methylene unit (Figure 1). It has been proposed that these antibiotics spontaneously insert into the plasma membrane of fungal cells and subsequently interact with fungal membrane sterols (mainly ergosterol) to form antibiotic−sterol complexes (*6*−*9*). These complexes then aggregate to generate membrane pores (*10*−*14*), which lead to cell lysis and cell death. The major problem with chemotherapy of amphotericin B and nystatin is that these antibiotics are quite toxic to human cells as a result of binding to membrane cholesterol, causing renal damage, and hemolytic anemia (*15*). Because of their toxicity, amphotericin B and nystatin cannot be given in sufficiently high doses to completely eradicate the fungal infections.

Although the antifungal activities and the cytotoxicity of nystatin and amphotericin B lie in their interactions with membrane sterols, little is known about the effect of sterol lateral organization on the actions of these polyene antibiotics. If, for example, sterols are segregated into domains in the membrane, formation of the antibiotic-induced membrane pores would occur instantaneously upon addition of antibiotics to cell membranes because, in this case, the time required for the lateral diffusion of antibiotic−sterol complexes to form membrane pores would be minimal. If, on the other hand, sterols are regularly distributed in the plane of the membrane, sterol molecules would be maximally separated (*16*). In this case, the formation of membrane pores would take a much longer time than the cases where sterols are either randomly distributed or domain segregated. Clearly,

[†] This work was supported in part by the American Heart Association (Grant 95010730) and in part by the Office of Naval Research (Grant N00 014-94-K-2005).

[‡] In memory of Professor Gregorio Weber.

* To whom correspondence should be addressed.

[§] Temple University School of Medicine.

[||] Mount Sinai Medical Center.

S0006-2960(98)00290-6 CCC: $15.00
Published on Web 08/07/1998

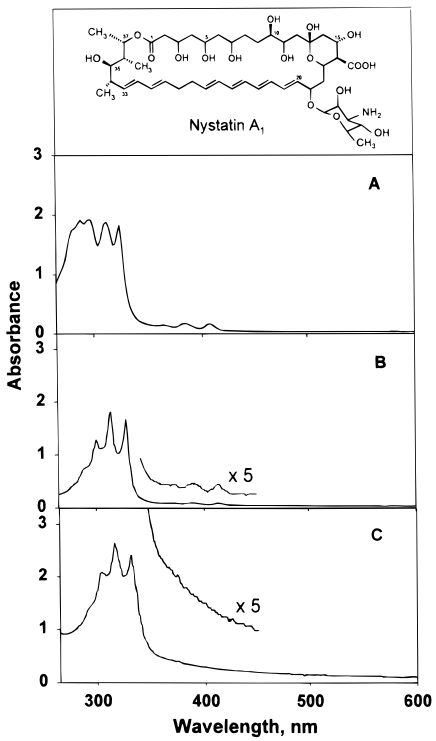

FIGURE 1: Absorption spectra of nystatin (A) from a commercial source and after (B) TLC and (C) HPLC purification.

the effect of sterol lateral organization on polyene antibiotics is an important issue and should be studied thoroughly.

In this work, we have addressed the above issue by using nystatin fluorescence to conduct a detailed study of the effects of membrane sterol content on the partitioning of nystatin into liquid-crystalline membrane bilayers. We have determined the partition coefficient of nystatin in ergosterol/dimyristoyl-L-α-phosphatidylcholine (DMPC[1]), cholesterol/DMPC, ergosterol/1-palmitoyl-2-oleoyl-L-α-phosphatidylcholine (POPC), and ergosterol/POPC/1-palmitoyl-2-oleoyl-L-α-phosphatidylethanolamine (POPE) multilamellar vesicles using ∼0.3−1.0 mol % sterol concentration increments over a wide sterol concentration range (e.g., 18−54 mol %). This unconventional approach of varying membrane sterol content, in contrast to previous studies using large sterol concentration increments (e.g., 10 mol % in ref *17* and 38 mol % in ref *18*), leads to a striking observation. The partitioning of nystatin changes with sterol content in a well-defined alternating manner, displaying a local minimum at the critical sterol mole fractions predicted for sterols regularly distributed in either hexagonal (*16*) or centered rectangular (*19*) superlattices. This phenomenon can be observed in both saturated (e.g., DMPC) and unsaturated (e.g., POPC) phosphatidylcholine lipid vesicles, and is persistent in the presence of polar headgroup heterogeneity (e.g., POPC/POPE). These results provide the semifunctional evidence supporting the sterol regular distribution model (*16*), demonstrate the importance of regular sterol distribution in nystatin partitioning to membranes, and point to a new method for studying the interactions of polyene antibiotics with sterol-containing membranes.

[1] Abbreviations: DMPC, dimyristoyl-L-α-phosphatidylcholine; POPC, 1-palmitoyl-2-oleoyl-L-α-phosphatidylcholine; POPE, 1-palmitoyl-2-oleoyl-L-α-phosphatidylethanolamine; MLVs, multilamellar vesicles.

MATERIALS AND METHODS

Materials. The concentrations of DMPC, POPC, and POPE (Avanti Polar Lipids, Alabaster, AL) were determined by the method of Bartlett (*20*). Ergosterol and cholesterol, obtained from Matreya (Pleasant, PA) and Sigma (St. Louis, MO), respectively, were recrystalized from ethanol.

Nystatin obtained from Sigma was first purified by thin-layer chromatography (TLC) on silica gel (150A, Whatman) using chloroform/methanol/water (20:22:10, v/v/v) (*21*). A band corresponding to nystatin (R_f = 0.75) was located by fluorescence, scraped, and eluted with methanol. The effluent was concentrated and further purified at ∼22 °C by high-performance liquid chromatography (HPLC) (model 324, Beckman, Berkeley, CA) with a C-18 reversed-phase column (3.9 mm × 300 mm, 10 μm Bondapak, Waters, Milford, MA) using a flow rate of 0.5 mL/min and linear gradient elution as described by Thomas et al. (*21*) with minor modifications. The first gradient elution started with 60% (v/v) methanol in 5 mM acetate buffer (pH 5.8) and ended with 100% methanol over the course of ∼30 min. Then the sample was eluted with 100% methanol for 10 min and followed by a second gradient from 100 to 60% (v/v) methanol in 5 mM acetate buffer (pH 5.8) over the course of 5 min. The purity of nystatin was verified by absorption spectra measured on a diode array spectrophotometer (model 8452A, Hewlett-Packard, Wilmington, DE). Commercially available nystatin from *Streptomyces nodosus* contains three tetraene antibiotics, i.e., A_1−A_3, with A_1 as the major component, and a small amount of amphotericin B (*22*). Nystatin A_1 and amphotericin B can be distinguished by their different absorption spectra. The characteristic absorption maxima of amphotericin B are 364, 383, and 408 nm (in ethanol), whereas the absorption maxima of nystatin A_1 are 292, 305, and 320 nm (in ethanol) (*23*). While the TLC-purified nystatin (Figure 1B) still contains a trace amount of amphotericin B, our HPLC-purified nystatin exhibits absorption maxima at 292, 304, and 320 nm in ethanol, without any detectable amphotericin B contamination (Figure 1C). The concentration of HPLC-purified nystatin was determined using an extinction coefficient at 304 nm equal to 74 000 M^{-1} cm^{-1} (in methanol) (*23*). A stock solution of nystatin in methanol (∼2 mM) was stored at −20 °C in the dark prior to being used.

Preparation of Liposomes. Multilamellar vesicles (MLVs) containing varying amounts of sterols were prepared as previously described (*16*, *24*, *25*). Appropriate amounts of sterols and phospholipids were first mixed in chloroform and then dried under nitrogen in microtubes (Perfector Scientific, Atascadero, CA), followed by further drying under high vacuum overnight. The dried mixtures were suspended in 100 mM Tris at pH 7.3 (measured at ∼22 °C). The dispersion was vortexed for 2 min at 45 °C to make MLVs. The MLVs were cooled to 4 °C for 30 min and then incubated at 45 °C for 30 min. This cooling−heating cycle was repeated two more times. Finally, the samples were stored at room temperature (∼22 °C) for at least 4 days prior to partitioning measurements. Heating−cooling cycles and long incubation provide a means of evenly distributing membrane components among lipid multilayers and attaining an equilibrium distribution of molecules within each monolayer (discussed in ref *25*).

Fluorescence Measurements. Fluorescence intensity measurements were made with a SLM DMX-1000 fluorometer (SLM Instruments, Urbana, IL). Samples were excited at 315 nm with a 1 nm band path. The emission was observed at 415 nm through a monochromator with an 8 nm band path. Since there is no significant difference in the final conclusion on the sterol dependence of nystatin partitioning before and after corrections of fluorescence intensities for light scattering from vesicles (Figure 4A) and since determination of light scattering contributions to all the sample readings would make this study excessively long, most of the partition coefficient data are presented without corrections for light scattering (open circles in Figures 3, 4A, 5, 6, and 7A).

Fluorescence lifetimes were determined using an ISS K2 phase-modulation fluorometer (*26*) (ISS, Inc., Champaign, IL). The light source was a He−Cd laser (model 4240NB, LiConix Inc., Sunnyvale, CA). The excitation wavelength was 325 nm. The excitation polarizer was set at 35° with respect to the vertical plane, and no emission polarizer was used. Phase and modulation values were determined relative to a *p*-bis[2-(5-phenyloxazolyl)]benzene (POPOP) (in ethanol) reference solution, which has a lifetime of 1.35 ns at 325 nm excitation (*27*). A Schott KV-389 cutoff filter was used for nystatin emission intensity decay measurements. The emission decay data was analyzed using the software provided by ISS Inc. For all the fluorescence measurements, the temperature of the sample was kept at 37 ± 0.2 °C by a circulating bath. At this temperature, all the bilayer membranes examined in this study are in the liquid-crystalline state.

Determination of the Partition Coefficient. The partition coefficient, *P*, defined as the relative molar ratio of nystatin in the membrane to that in the bulk solution, is described by the equation (*28*, *29*)

$$P = (S_l/L)/(S_w/W) = S_l W/S_w L \quad (1)$$

where S_l and S_w are the moles of nystatin in the membrane and in the bulk aqueous phase, respectively, and L and W are the moles of lipids and water in the sample, respectively. $S_l = [S_l]V_l$ and $S_w = [S_w]V_w$, where V_l is the volume of the membrane and V_w is the volume of the bulk aqueous solution. $W = 55.6V_w$, and $L = [L](V_w + V_l) \approx [L]V_w$ because, under our experimental conditions, $V_w \gg V_l$. The mole fraction of nystatin incorporated into the membrane X_l [$=S_l/(S_l + S_w)$] can thus be described as

$$X_l = [L]P/([L]P + 55.6) \quad (2)$$

Partitioning of nystatin from the aqueous phase into lipid membranes resulted in an increase in fluorescence intensity due to changes in quantum yield (*23*). When we assume that the fluorescence intensity increase is proportional to the amount of nystatin incorporated into lipid membranes, $X_l = (F - F_o)/(F_{max} - F_o) = \Delta F/\Delta F_{max}$, where F_o and F are the fluorescence intensities of nystatin in the absence and presence of lipid vesicles, respectively. F_{max} is the limiting value of F when the lipid concentration is very high. As a result (*28*),

$$\Delta F = \Delta F_{max}[L]/\{[L] + (55.6/P)\} \quad (3)$$

where [L] is the concentration of lipids (including sterols and phospholipids) that are available for nystatin binding. In this study, [L] is assumed to be 10% of the total lipid concentration in the sample, which is the amount of lipid in the outermost layer of multilamellar vesicles divided by V_w (*30*). The assumption that only the outermost layer is available for nystatin binding is justified as nystatin does not readily undertake transbilayer diffusion (*18*) and only the sterol in the outmost layer of multilamellar vesicles interacts with the polyene antibiotics (*31*). This assumption may become unnecessary if large unilamellar vesicles prepared by the extrusion method are used. However, extruded large unilamellar vesicles are more tedious to prepare. Also, a significant amount of lipids is usually retained by the extruder; as a result, additional determinations of [L] are required. Thus, for simplicity, this study is confined to MLVs.

Equation 3 allows us to determine the partition coefficient of nystatin in lipid membranes using steady-state fluorescence intensity, in a way similar to the method of Coutinho and Prieto (*23*). Specifically, for each sterol/phospholipid molar ratio examined, at least 16 samples with varying lipid concentrations were examined. To each of these samples was added a fixed amount of nystatin stock solution (in methanol), making the apparent final concentration of nystatin in the cuvette 5 μM. At this concentration, no nystatin self-association was detected in a liquid-crystalline lipid bilayer (*23*), and the amount of methanol in the sample (<0.3%) would not cause any appreciable perturbation in the bilayer (*23*). The nystatin-containing vesicles were then incubated for 1 h in the dark at 37 °C prior to fluorescence intensity measurements at 415 nm at the same temperature. The partition coefficient (*P*) at a given sterol/phospholipid molar ratio was determined using Kaleida Graph software (Synergy Software, Reading, PA) by fitting the data of the fluorescence intensity changes (ΔF) and the lipid concentrations ([L]) to eq 3. Under these experimental conditions, the final amount of nystatin present in membrane bilayers is small relative to that of membrane lipids (<0.5 mol % when $P < 300\,000$ and <1.2 mol % when $P > 360\,000$). Since there is no overlap between the absorption spectrum and the emission spectrum of nystatin, self-energy transfer due to nystatin aggregation in the bilayer does not occur (23). This means that drug localization has little effect on ΔF.

RESULTS

At a given sterol/phospholipid molar ratio, the enhancement of nystatin fluorescence intensity (ΔF) upon binding to sterol-containing lipid bilayer membranes varies with total lipid concentration [L] in a nonlinear manner, as illustrated in Figure 2. The dashed line of Figure 2 is the best fit of the data (i.e., ΔF and [L]) to eq 3, which yields a fitted partition coefficient of 311 930 ± 26 667 for 24.7 mol % ergosterol in DMPC MLVs at 37 °C. Using this method, we have determined the fractional ergosterol concentration dependence of the partition coefficient of nystatin into ergosterol/DMPC MLVs with ergosterol concentration increments of ~0.3−1.0 mol % over a wide ergosterol concentration range (18−54 mol %) (Figure 3). Ergosterol was chosen because it is the dominant sterol in fungal cell membranes. As shown in Figure 3, the partition coefficient, *P*, does not

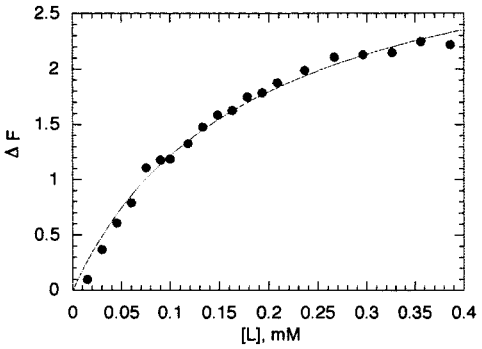

FIGURE 2: Typical data fitting curve for nystatin partitioning into ergosterol/DMPC MLVs at 37 °C. The data illustrate the enhancement of nystatin fluorescence intensity with increasing [L]. The dashed line is the best fit of the data to eq 3.

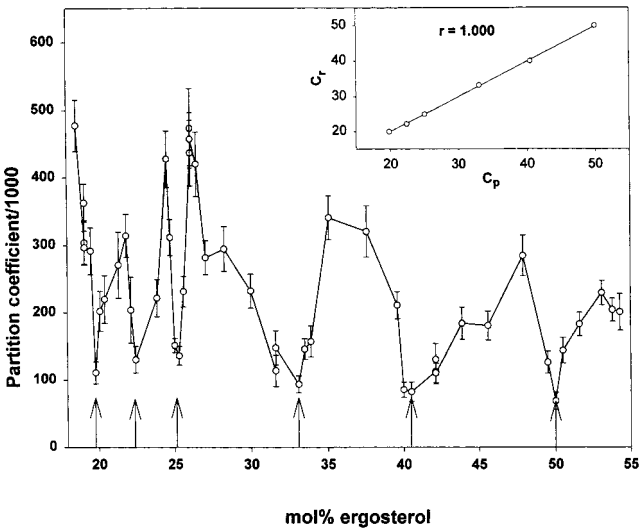

FIGURE 3: Effect of membrane ergosterol content on the partition coefficient of nystatin in ergosterol/DMPC MLVs at 37 °C. The inset depicts the correlation between the theoretically predicted sterol critical mole fractions (C_r) and the sterol mole fractions (C_p) at which the nystatin partition coefficient minima were observed. *r* is the correlation coefficient. The vertical bars are the standard deviations of the fitted partition coefficients.

change monotonically with ergosterol content; instead, *P* changes with sterol content in a well-defined alternating manner, reaching a local minimum at 19.8, 22.4, 25.0, 33.1, 40.5, and 50.0 mol % ergosterol (indicated by arrows in Figure 3). These ergosterol mole fractions agree, within the experimental errors (∼0.1−0.4 mol %; *16*, *25*), with the critical concentrations predicted for sterols regularly distributed in either extended hexagonal (i.e., 20.0, 25.0, 33.3, 40.0, and 50.0 mol % sterol; *16*, *25*) or centered rectangular (i.e., 20.0, 22.2, 33.3, 40.0, and 50.0 mol % sterol; *19*, *25*) superlattices. All of the six theoretically predicted critical mole fractions (20.0, 22.2, 25.0, 33.3, 40.0, and 50.0 mol % sterol) in the concentration range examined (18−54 mol % sterol) were shown to exhibit partitioning minima. Furthermore, partition coefficient minima were observed at, and only at, the theoretically predicted critical sterol mole fractions. A plot of the theoretically predicted critical sterol mole fractions versus the partition coefficient dip positions observed in ergosterol/DMPC bilayers gives an excellent correlation coefficient (*r*) of 1.000 (inset of Figure 3). The vertical bars in Figure 3 (as well as in Figures 4A, 5, and 6)

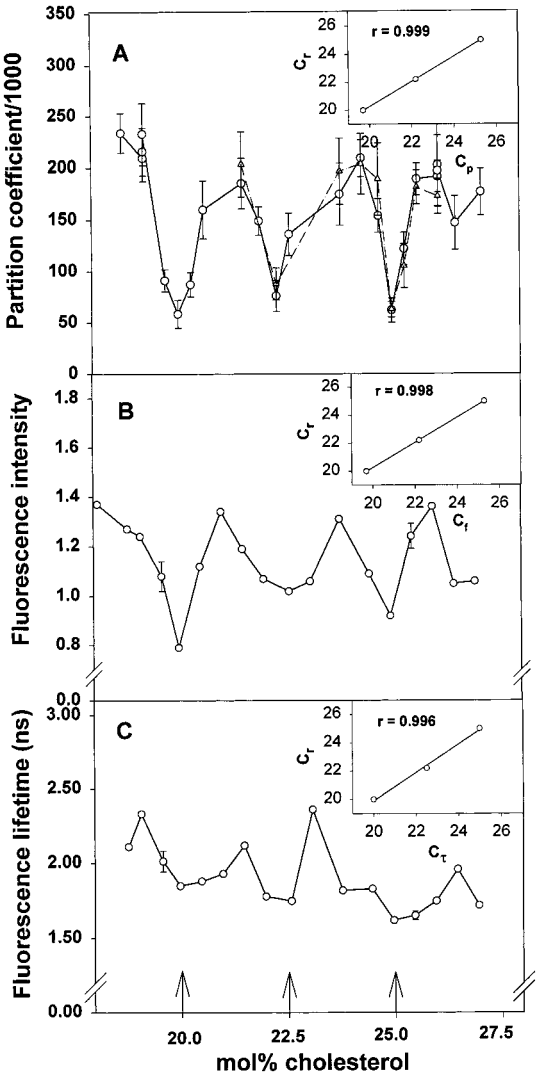

FIGURE 4: Effects of membrane cholesterol content on the partition coefficient of nystatin (A) and the intensity (B) and the average lifetime (C) of nystatin fluorescence in cholesterol/DMPC MLVs at 37 °C. The insets depict the correlations between the theoretically predicted sterol critical mole fractions (C_r) and the sterol mole fractions at which the nystatin partition coefficient minima (C_p), the intensity minima (C_f), and the lifetime minima (C_τ) were observed. The vertical bars in panel A are the standard deviations of the fitted partition coefficients, and the vertical bars in panels B and C represent the standard deviations resulting from three independently prepared samples. The open triangles in panel A are the partition coefficients determined using fluorescence intensities corrected for light scattering, whereas the open circles are not corrected for light scattering. The open triangles were determined as follows. At a given sterol/phospholipid molar ratio, two identical sets of vesicles with varying concentrations of L were prepared. One set was incubated with nystatin (sample); the other was not (blank). Both sets were measured under identical conditions. The blank readings were subtracted from the sample fluorescence readings. The fluorescence intensity corrected for light scattering from vesicles (designated as F_{corr}) as a function of [L] was fitted to a polynomial equation so that F_o (which is F_{corr} when [L] = 0) can be obtained. F_{corr} was then normalized using a fixed F_o value for all the sterol/phospholipid molar ratios examined. Partition coefficient *P* was determined with the equation $\Delta F = F_{corr,normalized} - F_o$ using eq 3.

are the standard deviations of the fitted partition coefficients. The horizontal axis of Figure 3 (as well as in Figures 4−6) indicates the sterol mole percentages in the membranes prior to addition of nystatin.

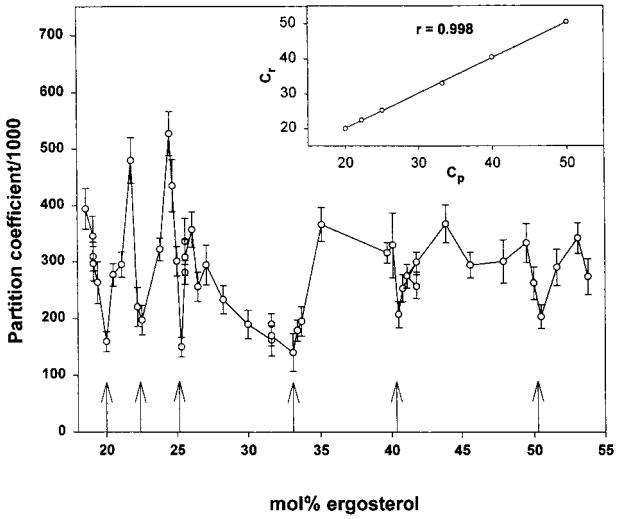

FIGURE 5: Effect of membrane ergosterol content on the partition coefficient of nystatin in ergosterol/POPC MLVs at 37 °C. The inset depicts the correlation between the theoretically predicted sterol critical mole fractions (C_r) and the sterol mole fractions (C_p) at which the nystatin partition coefficient minima were observed. *r* is the correlation coefficient. The vertical bars are the standard deviations of the fitted partition coefficients.

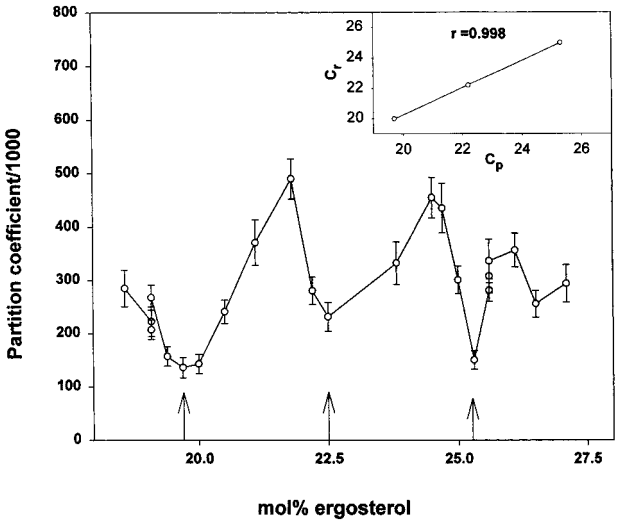

FIGURE 6: Effect of membrane ergosterol content on the partition coefficient of nystatin in ergosterol/POPC/POPE MLVs at 37 °C. The molar ratio of POPC/POPE was equal to 1 in all the samples. The inset depicts the correlation between the theoretically predicted sterol critical mole fractions (C_r) and the sterol mole fractions (C_p) at which the nystatin partition coefficient minima were observed. *r* is the correlation coefficient. The vertical bars are the standard deviations of the fitted partition coefficients.

A similar alternating pattern is seen in the plot of nystatin partition coefficient versus cholesterol mole fraction in cholesterol/DMPC MLVs at 37 °C (Figure 4A). The interest of studying cholesterol lies in the fact that nystatin also binds to cholesterol in the membrane of human cells, causing cytotoxicity (*1*, *15*). In this experiment, a smaller sterol concentration range (18−27 mol %) was examined; still, three partition coefficient minima were detected at 20.0, 22.3, and 25.0 mol % cholesterol. These concentrations are at or close to the critical sterol mole fractions (correlation coefficient $r = 0.999$; inset of Figure 4A) for the formation of hexagonal or centered rectangular superlattices, as mentioned earlier. It is also interesting to note that at a given sterol mole fraction the partition coefficient of nystatin in cholesterol/DMPC bilayers (Figure 4A) is lower than that in ergosterol/DMPC mixtures (Figure 3). This trend is consistent with the previous finding that nystatin or amphotericin B interacts more strongly with membrane ergosterol than membrane cholesterol (*17*, *32*−*34*).

The open triangles in Figure 4A are the partition coefficients determined using fluorescence intensities corrected for light scattering from vesicles, whereas the open circles are not corrected for light scattering. Both determinations give similar results showing a sharp partition coefficient dip at 25 mol % (Figure 4A). This clearly demonstrates that light scattering from vesicles does not cause significant changes in the alternating variation of nystatin partitioning with membrane sterol content.

Parallel with the alternating variation of nystatin partition coefficient with cholesterol content are the periodic variations of nystatin fluorescence intensity (Figure 4B). The nystatin fluorescence intensity exhibits sharp dips at 20.0, 22.5, and 25.0 mol % cholesterol (Figure 4B). The effect of cholesterol content on the average lifetime, $\langle\tau\rangle$, of nystatin fluorescence in cholesterol/DMPC MLVs at 37 °C was also examined (Figure 4C). The nystatin fluorescence lifetime was determined by phase and modulation measurements using modulation frequencies ranging from 60 to 200 MHz. The data are best fit by a two-exponential decay law, $F(t) = \alpha_1 \exp(-t/\tau_1) + \alpha_2 \exp(-t/\tau_2)$, where α_i and τ_i are the preexponential factor and lifetime, respectively, for the *i*th component. The average lifetime $\langle\tau\rangle$ was calculated from the equation $\langle\tau\rangle = f_1\tau_1 + f_2\tau_2$, where f_i is the fraction of the total fluorescence intensity derived from the *i*th component [$f_1 = \alpha_1\tau_1/(\alpha_1\tau_1 + \alpha_2\tau_2)$ and $f_2 = 1 - f_1$]. Like the fluorescence intensity data (Figure 4B), the average fluorescence lifetime $\langle\tau\rangle$ (Figure 4C) also exhibits dips at 20.0, 22.5, and 25.0 mol % cholesterol. These concentrations are identical or close to the theoretical values predicted for sterol regular distribution in hexagonal and/or centered rectangular superlattices (*16*, *19*, *25*, *35*, *36*). The observation that the intensity and the lifetime of nystatin fluorescence reach a local minimum at critical sterol mole fractions is expected because fewer nystatin molecules insert into the bilayer at critical mole fractions (Figure 4A) and the quantum yield of nystatin fluorescence in water is lower than that in the membrane (*23*).

The alternating variation of nystatin partitioning with sterol content is also evident in ergosterol/POPC MLVs at 37 °C (Figure 5). In this case, the partitioning minima can be observed at 20.0, 22.5, 25.3, 33.1, 40.5, and 50.5 mol % ergosterol (indicated by arrows in Figure 5). These concentrations are consistent with the critical sterol mole fractions predicted for superlattice formation ($r = 0.998$; inset of Figure 5). Figure 6 shows the fractional ergosterol concentration dependence of nystatin partitioning in ergosterol/POPC/POPE MLVs (the molar ratio of POPC to POPE equals 1) at 37 °C. In the ergosterol concentration range examined, three distinct partition coefficient dips were noticed at 19.7, 22.2, and 25.3 mol % ergosterol. Again, these concentrations conincide with the theoretical values for maximal superlattice formation ($r = 0.996$; inset of Figure 6), showing that the periodic variation of nystatin partitioning with membrane sterol content persists in the presence of polar headgroup heterogeneity.

DISCUSSION

The alternating variation of the partition coefficient of nystatin with membrane sterol content in a well-defined pattern (Figures 3−6) is a remarkable finding. At present, this phenomenon can only be understood by the sterol regular distribution model (*16*, *25*, *35*, *36*). The sterol regular distribution model states that regularly distributed lipid superlattices coexist with irregularly distributed lipid areas in the plane of sterol-containing membranes and that the ratio of regular to irregular distributions reaches a local maximum at critical sterol mole fractions (*37*). In the range of 18−54 mol % sterol, six critical sterol mole fractions (20.0, 22.2, 25.0, 33.0, 40.0, and 50.0 mol % sterol) are predicted for maximal formation of superlattices (*16*, *19*, *25*, *38*, *39*). The partition coefficient minima observed in this study (Figures 3−6) are consistent with these theoretical values, thus suggesting that the partitioning of nystatin into liquid-crystalline phospholipid membranes is minimal when the extent of sterol superlattices in the plane of the membrane is maximal.

The sterol regular distribution model also states that the membrane free volume varies with sterol content in an alternating manner, with the smallest membrane free volume present at critical sterol mole fractions where the extent of superlattices is maximal (*25*, *35*, *36*, *40*, *41*). Note that partitioning of hydrophobic solutes, such as hexane (*42*) and benzene (*43*), into membranes has previously been demonstrated to decrease with decreasing membrane free volume, and this property may also apply to the partitioning of nystatin. Thus, the observation that nystatin partitioning is minimal at critical sterol mole fractions (Figures 3−6) can be understood in terms of changes in membrane free volume via changes in the extent of lipid superlattices.

In the context of sterol regular distribution, one can assume that the packing of the lipid molecules is so perfect at the areas of regular distribution that there is no room for nystatin binding, but at the areas of irregular sterol distribution, nystatin binding to the membrane increases with increasing sterol concentration. At low sterol concentrations (e.g., <5 mol %), the regularly distributed sterol molecules would be separated from each other by a large distance in the lipid matrix. In this case, regular distribution is practically not existent. It is found that at these low ergosterol concentrations (0−5 mol %) the partition coefficient of nystatin into ergosterol/DMPC bilayers indeed increases linearly with increasing ergosterol content (Figure 7A). The partition coefficients of nystatin in the absence of regular distribution are designated as P_o. The linear plot shown in Figure 7A allows us to extrapolate the P_o values at high ergosterol concentrations (e.g., 18−54 mol %) where appreciable amounts of regular distributions are believed to coexist with irregular distributions. Using these extrapolated P_o values and the partition coefficients (P) presented in Figure 3, the proportion of the membrane surface area, A_{reg}, covered by regularly distributed lipid molecules can be calculated via eq A4 (Appendix). As shown in Figure 7B, A_{reg} in ergosterol/DMPC MLVs at 37 °C varies with membrane ergosterol content in an alternating manner, exhibiting a local maximum at 19.8, 22.4, 25.0, 33.1, 40.5, and 50.0 mol % ergosterol. These concentrations are consistent with the critical sterol mole fractions predicted by the extended hexagonal and/or the centered rectangular superlattice models. At all the concentrations examined, A_{reg} is less than 90% of the total membrane surface area, and A_{reg} may change abruptly by a factor of 2 from a critical sterol mole fraction to one of the adjacent noncritical mole fractions (Figure 7B). The A_{reg} results are in parallel with the partitioning data shown in Figure 3, fully supporting the suggestion that nystatin partitioning is regulated by the extent of sterol regular distribution in the membrane. It is interesting to note that the assumption that nystatin partitions only in the irregular region is compatible with the freeze-fracture electron micrographs of the plasma membranes of fungal cells *Epidermophyton floccosum* and *Saccharomyces cerevisiae* treated with nystatin and amphotericin B, where membrane particles aggregate into small particle islands surrounded by wide particle-free areas (*44*).

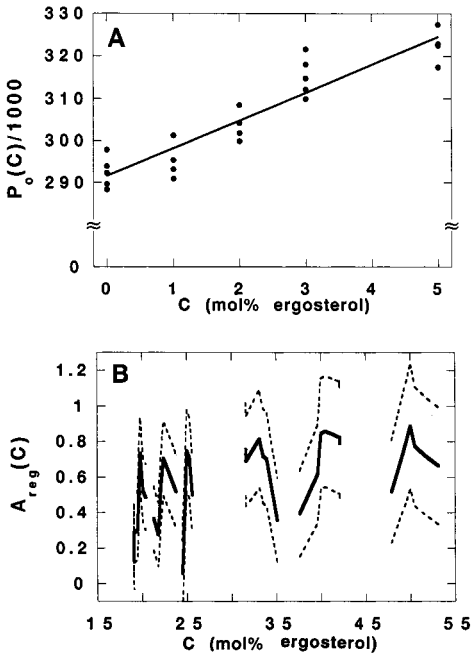

FIGURE 7: (A) Ergosterol concentration dependence of the partition coefficient of nystatin into ergosterol/DMPC MLVs in the ergosterol concentration range of 0−5 mol % at 37 °C. The solid line is the linear regression of 22 experimental points (n = 22) with a correlation coefficient r of 0.93. (B) Area of regular ergosterol distribution relative to the total outermost membrane surface (A_{reg}) plotted against ergosterol content in ergosterol/DMPC MLVs at 37 °C. The solid lines are the expected values of A_{reg} calculated by using eq A4; the dotted lines are the standard deviations, $\sigma_{A_{reg}(C)}$, from the expected values of A_{reg} calculated by using eq A5. The local maximal values of A_{reg} are 0.74 ± 0.20 at 19.8 mol %, 0.71 ± 0.21 at 22.4 mol %, 0.75 ± 0.23 at 25.0 mol %, 0.81 ± 0.28 at 33.1 mol %, 0.86 ± 0.31 at 40.5 mol %, and 0.89 ± 0.35 at 50.0 mol % ergosterol.

All the present findings greatly strengthen the conceptual framework of sterol regular distribution. Previous evidence for sterol regular distribution was almost exclusively based on spectroscopic parameters such as fluorescence intensities (*16*, *19*, *45*, *46*), fluorescence lifetimes (*25*, *35*, *36*), fluorescence anisotropies (*25*, *35*, *36*, *41*), light scattering signals (*19*), absorption (*19*), and the fluorescence quenching rate constant (*35*, *36*). This study demonstrates an excellent agreement between the sterol regular distribution model and the experimental data by virtue of a membrane property (i.e., partition coefficient), rather than a spectroscopic parameter. This rules out the possibility that sterol regular distribution

is a result of spectroscopic artifacts. More importantly, these partitioning data, along with the results of the hydrolytic activity of secreted phospholipase A2 (*47*), are consistent with the earlier prediction (*25*, *40*) that membrane properties known to be influenced by membrane free volume will be altered by sterol content in a periodic manner, showing biphasic changes at critical sterol mole fractions. Recall that the fluorescence quenching data (*35*, *36*) also are consistent with the prediction (*16*) that sterol molecules in the regularly distributed lipid areas are more exposed to the aqueous phase than sterols in the irregularly distributed areas. All these agreements make an important point that although at present the sterol regular distribution model has not been proven by direct structural measurements such as X-ray diffraction and atomic force microscopy, all the membrane properties predicted by the model have been demonstrated to be correct (refs *25*, *35*, *36*, and *47* and this study). In addition, evidence for sterol regular distribution has previously been obtained in liquid-crystalline DMPC (*16*, *19*, *25*, *35*, *36*, *41*, *45*), DPPC (*25*), and sphingomyelin (*35*, *36*) bilayers. Here we have extended the work to POPC and POPC/POPE MLVs. POPC and POPE are abundant in mammalian cell membranes, and they have a double bond between C9 and C10 in the *sn*-2 acyl chain. The excellent agreement between the partition coefficient dips (Figures 5 and 6) and the theoretically predicted critical sterol mole fractions provide evidence, for the first time, that sterol regular distribution also occurs in unsaturated lipid bilayers and that nystatin partitioning is modulated by the extent of sterol superlattice in both saturated (DMPC) and unsaturated lipid bilayers. The fact that evidence for sterol regular distribution exists in so many different phospholipid model membrane systems as revealed and tested by various techniques and methods convinces us that this phenomenon must be real and that the sterol regular distribution model is a working model. All these results also support the possibility that sterol regular distribution may exist in real biological membranes. In sterol/sphingolipid- or sterol/phosphatidylcholine-enriched domains of biological membranes (e.g., detergent-insoluble, sphingolipid/cholesterol rafts in cell membranes; *48*, *49*), lipids are likely to be regularly distributed as superlattices, in coexistence with irregularly distributed regions (as depicted in ref *25*).

The striking new finding revealed in this study has profound biological and pharmaceutical implications. First, our data (Figures 3−6) show that the partition coefficient of nystatin in lipid membranes can vary dramatically with a minute change (e.g., 1 mol %) in membrane sterol content in the vicinity of a critical sterol mole fraction predicted for maximal formation of sterol superlattices. For example, the partition coefficient of nystatin increases by a factor of 4 from 25.0 (a critical sterol mole fraction) to 26.0 mol % ergosterol (a noncritical mole fraction) in ergosterol/DMPC MLVs (Figure 3). This phenomenon suggests that there is a need to consider the membrane sterol content and the extent of sterol superlattice in the membranes of the target cells when administering nystatin or other polyene antibiotics. The drug uptake by a target cell membrane should in principle reach a local minimum when the sterol content in the target cell membrane is at one of the critical sterol mole fractions, and a local maximum when the membrane sterol content is between two consecutive critical sterol mole fractions. Second, since membrane partitioning is the first step of the antifungal action of nystatin or other polyene antibiotics, it is a possibility that the subsequent actions of polyene antibiotics, such as pore formation and membrane leakage, would also be affected by membrane sterol content via changes in the extent of sterol superlattice. As such, these data (Figures 3−6) call attention to the fact that previous works on the relationship between membrane sterol concentration and the molecular actions of polyene antibiotics need to be re-examined by using small sterol concentration increments (e.g., ∼0.3 mol %). Third, the cytotoxicity of nystatin or amphotericin B can be greatly reduced by using liposomal delivery systems (*50*−*55*), many of which include cholesterol and phospholipids as the major components. Then, the concept derived from this study may be used to refine the molar ratio of cholesterol to phospholipids in the liposomal formulations to attain an optimal fungicidal activity. The final point is that these results may be generally applicable because solute partitioning is the basis of the actions of many other drugs (*56*), lipophilic insecticides (*57*), intracellular lipid and protein trafficking (*58*), and passive transport of metabolites across cellular membranes.

ACKNOWLEDGMENT

We are grateful to Drs. P. Walsh and F. London for discussions and for use of their spectrophotometer. I.P.S. acknowledges Ms. L. Garner for general support.

APPENDIX

Estimation of A_{reg}

If A_{reg} is the proportion of the membrane surface area where the sterol molecules are regularly distributed and C_{cr} is the sterol concentration at the areas of regular distribution, then

$$A_{reg}C_{cr} + (1 - A_{reg})C_{irreg} = C \qquad \text{(A1)}$$

where C is the total sterol concentration in the membrane and C_{irreg} is the sterol concentration at the areas of irregular sterol distribution. Equation A1 assumes that C is sufficiently close to a critical concentration C_{cr}, and thus, the sterol concentration in the areas of regular sterol distribution is equal to C_{cr}. Note that without this constraint it is possible that two types of regularly distributed domains coexist, one with a sterol concentration $C_{cr,low}$ that is less than C and another $C_{cr,high}$ that is greater than C.

At low sterol concentrations (C < 5 mol %), the sterol molecules are virtually irregularly distributed ($A_{reg} \approx 0$) in the lipid matrix of the membrane, and the partition coefficient of nystatin increases linearly with increasing concentration (Figure 7A)

$$P_o(C) = P_o(0) + aC \qquad \text{(A2)}$$

The estimated parameters of the regression line (Figure 7A) obtained from ergosterol/DMPC MLVs at 37 °C are as follows: $P_o(0) = 291\,550 \pm 1580$ and the slope of the fitted line $a = 6590 \pm 580$ (mol %)$^{-1}$.

At higher sterol concentrations (C > 5 mol %), especially at the critical concentrations, $A_{reg} > 0$. Assume that the packing of the lipid molecules is so perfect at the areas of

regular distribution that there is no room for nystatin binding, while in the areas of irregular distribution the linear relationship, given by eq A2, is valid. Thus, the partition coefficient of nystatin is

$$P(C) = P_o(C_{irreg})[1 - A_{reg}(C)] \quad \text{(A3)}$$

By using eq A1, one can eliminate C_{irreg} from eq A3 and obtain A_{reg} as follows

$$A_{reg}(C) = [P_o(C) - P(C)]/P_o(C_{cr}) \quad \text{(A4)}$$

By means of the variance propagation, the variance of A_{reg} is

$$\sigma^2 A_{reg}(C) = A_{reg}{}^2 \sigma^2_{P_o(C_{cr})}/[P_o(C_{cr})]^2 + [\sigma^2_{P_o(C)} + \sigma^2_{P(C)}]/[P_o(C_{cr})]^2 \quad \text{(A5)}$$

The standard deviations of the partition coefficients measured at different ergosterol mole fractions do not show systematic concentration dependence (e.g., Figure 3); thus, it can be estimated by the average of the standard deviations $\sigma_{P(C)}$ (=26800). The variance of the partition coefficient P_o, however, has a strong concentration dependence. The partition coefficient P_o at high ergosterol mole fractions, C, is approximated from the P_o values observed at low ergosterol mole fractions of C_1, C_2, ..., C_i, ..., C_n. The variance of P_o increases with increasing ergosterol concentration, C, as follows (*59*):

$$\sigma^2_{P_o(C)} = \sigma^2_{P(C)}\{1 + 1/n + [(C - C_{av})^2]/\sum_{i=1}^{n}(C_i - C_{av})^2\} \quad \text{(A6)}$$

where $C_{av} = (1/n)\sum_{i=1}^{n} C_i$. It is important to note that the estimated A_{reg} values are less reliable at higher sterol concentrations because the standard deviation is larger and also because the extrapolation of the linear relationship in eq A2 is less reliable at higher C values. By increasing n, which is the number of P_o data obtained from measurements at low ergosterol concentrations, one can decrease the variance of $P_o(C)$ and $A_{reg}(C)$ to a predefined level, while the expected value of $A_{reg}(C)$ does not change significantly (Figure 7B).

REFERENCES

1. Medoff, G., Brajtburg, J., Kobayashi, G. S., and Bolard, J. (1983) *Annu. Rev. Pharmacol. Toxicol. 23*, 303−330.
2. Bolard, J. (1986) *Biochim. Biophys. Acta 864*, 257−304.
3. Finkelstein, A. (1987) in *Water Movement Through Lipid Bilayers, Pores, and Plasma Membranes*, Chapter 7, pp 107−129, John Wiley and Sons, New York.
4. Warnock, D. W. (1991) *J. Antimicrob. Chemother. 28*, 27−38.
5. Wallace, T. L., Paetznick, V., Cossum, P. A., Lopez-Berestein, G., Rex, J. H., and Anaissie, E. (1997) *Antimicrob. Agents Chemother. 41*, 2238−2243.
6. De Kruijff, B., and Demel, R. A. (1974) *Biochim. Biophys. Acta 339*, 57−70.
7. van Hoogevest, P., and De Kruijff, B. (1978) *Biochim. Biophys. Acta 511*, 397−407.
8. vanden Bossche, H., Wollensens, G., and Marichal, P. (1987) *Crit. Rev. Microbiol. 15*, 57−72.
9. Haynes, M. P., Chong, P. L.-G., Buckley, H. R., and Pieringer, R. A. (1996) *Biochemistry 35*, 7983−7992.
10. Holz, R., and Finkelstein, A. (1970) *J. Gen. Physiol. 56*, 125−145.
11. Finkelstein, A., and Holz, R. (1973) in *Membrane Lipid Bilayers and Antibiotics* (Eisenman, G., Ed.) p 377, Marcel Dekker, New York.
12. Andreoli, T. E. (1974) *Ann. N.Y. Acad. Sci. 235*, 448−468.
13. Brajtburg, J., Powderly, W. G., Kobayashi, G. S., and Medoff, G. (1990) *Antimicrob. Agents Chemother. 34*, 183−188.
14. Fujii, G., Chang, J.-E., Coley, T., and Steere, B. (1997) *Biochemistry 36*, 4959−4968.
15. Kinsky, S. C. (1967) in *Antibiotics* (Gottlieb, D., and Shaw, P. D., Eds.) Vol. 1, pp 122−141, Springer-Verlag, New York.
16. Chong, P. L.-G. (1994) *Proc. Natl. Acad. Sci. U.S.A. 91*, 10069−10073.
17. Teerlink, T., De Kruijff, B., and Demel, R. A. (1980) *Biochim. Biophys. Acta 599*, 484−492.
18. Abramson, M. B., and Ockman, N. (1973) *J. Colloid Interface Sci. 43*, 530−538.
19. Virtanen, J. A., Ruonala, M., Vauhkonen, M., and Somerharju, P. (1995) *Biochemistry 34*, 11568−11581.
20. Bartlett, G. R. (1959) *J. Biol. Chem. 234*, 466−468.
21. Thomas, A. H., Pharm, B., Newland, P., and Quinlan, G. J. (1981) *J. Chromatogr. 216*, 367−373.
22. Kleinberg, M. E., and Finkelstein, A. (1984) *J. Membr. Biol. 80*, 257−269.
23. Coutinho, A., and Prieto, M. (1995) *Biophys. J. 69*, 2541−2557.
24. Kao, Y. L., Chong, P. L.-G., and Huang, C. (1990) *Biochemistry 29*, 1315−1322.
25. Liu, F., Sugar, I. P., and Chong, P. L.-G. (1997) *Biophys. J. 72*, 2243−2254.
26. Gratton, E., and Limkeman, M. (1983) *Biophys. J. 44*, 315−324.
27. Lakowicz, J. R., Cherek, H., and Balter, A. (1981) *J. Biochem. Biophys. Methods 5*, 131−146.
28. Huang, Z., and Haugland, R. P. (1991) *Biochem. Biophys. Res. Commun. 181*, 166−171.
29. Welti, R., Mullikin, L. J., Yoshimura, T., and Helmkamp, G. M. (1984) *Biochemistry 23*, 6086−6091.
30. Cullis, P. R., and Hope, M. J. (1985) in *Biochemistry of Lipids and Membranes* (Vance, D. E., and Vance, J. E., Eds.) p 36, Benjamin/Cummings Publishing Company, Inc., Menlo Park, CA.
31. De Kruijff, B., Gerritsen, W. J., Oerlemans, A., Demel, R. A., and Van Deenen, L. L. M. (1974) *Biochim. Biophys. Acta 339*, 30−43.
32. Gale, E. F. (1974) *J. Gen. Microbiol. 80*, 451−465.
33. Readio, J. D., and Bittman, R. (1982) *Biochim. Biophys. Acta 685*, 219−224.
34. Vertut-Croquin, A., Bolard, J., Chabbert, M., and Gary-Bobo, C. (1983) *Biochemistry 22*, 2939−2944.
35. Chong, P. L.-G., Wang, M. M., Liu, F., Truong, K., Golsorkhi, A. A., Sugar, I. P., and Brown, R. E. (1996) *Proceedings of Fluorescence Detection IV, SPIE*, Vol. 2705, pp 143−154.
36. Chong, P. L.-G., Liu, F., Wang, M. M., Truong, K., Sugar, I. P., and Brown, R. E. (1996) *J. Fluoresc. 6*, 221−230.
37. Sugar, I. P., Tang, D., and Chong, P. L.-G. (1994) *J. Phys. Chem. 98*, 7201−7210.
38. Virtanen, J. A., Somerharju, P., and Kinnunen, P. K. J. (1988) *J. Mol. Electron. 4*, 233−236.
39. Tang, D., and Chong, P. L.-G. (1992) *Biophys. J. 63*, 903−910.
40. Chong, P. L.-G., Tang, D., and Sugar, I. P. (1994) *Biophys. J. 66*, 2029−2038.
41. Chong, P. L.-G. (1996) in *High-Pressure Effects in Molecular Biophysics and Enzymology* (Markley, J. L., Northrop, D. B., and Royer, C. A., Eds.) pp 298−313, Oxford University Publishing, New York.
42. De Young, L. R., and Dill, A. (1990) *J. Phys. Chem. 94*, 801−809.

43. De Young, L. R., and Dill, A. (1988) *Biochemistry 27*, 5281−5289.
44. Kitajima, Y., Sekiya, T., and Nozawa, Y. (1976) *Biochim. Biophys. Acta 445*, 452−465.
45. Parasassi, T., Giusti, A. M., Raimondi, M., and Gratton, E. (1995) *Biophys. J. 68*, 1895−1902.
46. Tang, D., van der Meer, W. B., and Chen, S.-Y. S. (1995) *Biophys. J. 68*, 1944−1951.
47. Liu, F., and Chong, P. L.-G. (1997) *Biophys. J. 72*, A71.
48. Brown, D. A., and Rose, J. K. (1992) *Cell 68*, 533−544.
49. Simons, K., and Ikonen, E. (1997) *Nature 387*, 569−572.
50. Lopez-Berestein, G., Mehta, R., Hopfer, R. L., Mills, K., Kasi, L., Mehta, K., Fainstein, V., Luna, M., Hersh, E. M., and Juliano, R. (1983) *J. Infect. Dis. 147*, 939−945.
51. Mehta, R. T., Hopfer, R. L., McQueen, T., Juliano, R. L., and Lopez-Berestein, G. (1987) *Antimicrob. Agents Chemother. 31*, 1901−1903.
52. Szoka, F. C., Milholland, D., and Barza, M. (1987) *Antimicrob. Agents Chemother. 31*, 421−429.
53. Janoff, A. S., Boni, L. T., Popescu, M. C., Minchey, S. R., Cullis, P. R., Madden, T. D., Taraschi, T., Gruner, S. M., Shyamsunder, E., Tate, M. W., Mendelsohn, R., and Bonner, D. (1988) *Proc. Natl. Acad. Sci. U.S.A. 85*, 6122−6126.
54. Adler-Moore, J. P., and Proffitt, R. T. (1993) *J. Liposome Res. 3*, 429−450.
55. Hartsel, S., and Bolard, J. (1996) *Trend. Pharm. Sci. 17*, 445−449.
56. Samuni, A., Chong, P. L.-G., Barenholz, Y., and Thompson, T. E. (1986) *Cancer Res. 46*, 594−599.
57. Antunes-Madeira, M. C., and Madeira, V. M. C. (1986) *Biochim. Biophys. Acta 861*, 159−164.
58. Scheiffele, P., Roth, M. G., and Simons, K. (1997) *EMBO J. 16*, 5501−5508.
59. Neter, J., and Wasserman, W. (1974) in *Applied Linear Statistical Model*, p 66, Richard D. Irwine, Inc., Homewood, IL.

BI980290K